VIPP1 Has a Disordered C-Terminal Tail Necessary for Protecting Photosynthetic Membranes against Stress[1][OPEN]

Lingang Zhang, Hideki Kondo, Hironari Kamikubo, Mikio Kataoka, and Wataru Sakamoto*

Institute of Plant Science and Resources, Okayama University, Kurashiki, Okayama 710-0046, Japan (L.Z., H.Ko., W.S.); School of Life Science and Technology, Inner Mongolia University of Science and Technology, Baotou 014010, China (L.Z.); and Graduate School of Materials Science, Nara Institute of Science and Technology, Ikoma, Nara 630-0101, Japan (H.Ka., M.K.)

ORCID IDs: 0000-0002-0878-6488 (H.Ka.); 0000-0001-6456-6394 (M.K.); 0000-0001-9747-5042 (W.S.).

Integrity of biomembranes is vital to living organisms. In bacteria, PspA is considered to act as repairing damaged membrane by forming large supercomplexes in Arabidopsis (*Arabidopsis thaliana*). Vulnerable to oxidative stress, photosynthetic organisms also contain a PspA ortholog called VIPP1, which has an additional C-terminal tail (Vc). In this study, Vc was shown to coincide with an intrinsically disordered region, and the role of VIPP1 in membrane protection against stress was investigated. We visualized VIPP1 by fusing it to GFP (VIPP1-GFP that fully complemented lethal *vipp1* mutations), and investigated its behavior in vivo with live imaging. The intrinsically disordered nature of Vc enabled VIPP1 to form what appeared to be functional particles along envelopes, whereas the deletion of Vc caused excessive association of the VIPP1 particles, preventing their active movement for membrane protection. Expression of VIPP1 lacking Vc complemented *vipp1* mutation, but exhibited sensitivity to heat shock stress. Conversely, transgenic plants over-expressing VIPP1 showed enhanced tolerance against heat shock, suggesting that Vc negatively regulates VIPP1 particle association and acts in maintaining membrane integrity. Our data thus indicate that VIPP1 is involved in the maintenance of photosynthetic membranes. During evolution, chloroplasts have acquired enhanced tolerance against membrane stress by incorporating a disordered C-terminal tail into VIPP1.

Living organisms depend on biomembranes for their survival. Biomembranes separate cells from the outer environment. Inside the cell, the membrane constitutes elaborate subcomponents as organelles by controlling trafficking of organic and inorganic compounds. Loss of membrane integrity impairs growth and cell viability because it engenders disturbances in electric membrane potential and proton-motive force. To protect membranes from damage, living organisms have developed elaborate methods by which membrane disruption can be repaired rapidly. In bacteria, a series of genes (*Psp*) are activated against phage shock stress, i.e. the membrane damage caused by phage infection and other membrane stresses. PspA forms large homo-oligomeric annular supercomplexes possibly used to repair ruptured membranes (Kleerebezem et al., 1996; Kobayashi et al., 2007; Standar et al., 2008), although its precise role in mitigating membrane damage remains elusive.

Most organisms performing oxygenic photosynthesis have a PspA homolog designated as Vesicle Inducing Protein in Plastid 1 (VIPP1; Kroll et al., 2001). Multiple functions of VIPP1 have been proposed, including vesicle induction (Kroll et al., 2001), photosynthetic protein supercomplex formation (Nordhues et al., 2012), reorganization of the thylakoid structure (Lo and Theg, 2012), photosystem I biogenesis in *Synechococcus* sp. PCC 7002 (Zhang et al., 2014), membrane fusion (Hennig et al., 2015), and membrane stabilization (McDonald et al., 2015). Moreover, our study highlighted another function of VIPP1: chloroplast envelope membrane protection (Zhang et al., 2012).

Chloroplasts, originating from cyanobacterial endosymbiosis, maintain their integrity through the envelope membrane, which is susceptible to environmental stresses such as heat and drought (McCain et al., 1989; Dekov et al., 2000). The integrity of thylakoid membranes is also crucially important for photosynthesis and chloroplast functions. We found previously that mesophyll cells in *vipp1* mutants exhibit swollen chloroplasts that result from impaired response of envelopes to hypotonic membrane stress (Zhang et al., 2012). Moreover, our previous live-imaging demonstrated that in chloroplasts, large VIPP1 complexes associated with the inner

[1] This work was partly supported by the Japan Science and Technology Agency (Core Research for Evolutional Science and Technology to W.S.), the Ministry of Education, Culture, Sports, Science and Technology (Grant-in-Aid from the NC-CARP project to W.S.), and the Ohara Foundation (to W.S.).

* Address correspondence to saka@okayama-u.ac.jp.

The author responsible for distribution of materials integral to the findings presented in this article in accordance with the policy described in the Instructions for Authors (www.plantphysiol.org) is: Wataru Sakamoto (saka@okayama-u.ac.jp.).

L.Z. performed most of the experiments, analyzed data, and wrote the manuscript; H.Ko., H.Ka., and M.K. provided technical assistance to L.G.; W.S. conceived the research project, designed and performed the experiments, and wrote the manuscript with contributions of all authors.

[OPEN] Articles can be viewed without a subscription.

www.plantphysiol.org/cgi/doi/10.1104/pp.16.00532

envelope displayed dynamic behavior responding to hypotonic stress: disassembled VIPP1 began to move rapidly within swollen stroma and appeared to reassemble on the envelope in a filament-like structure. These observations, along with those of other reports (Zhang and Sakamoto, 2013; 2015; Hennig et al., 2015), corroborate the important role of VIPP1 in photosynthetic membrane integrity. Movement associated with membrane stress has also been reported in PspA (Engl et al., 2009; Yamaguchi et al., 2013).

This report describes the extraordinary capacity of VIPP1 to protect chloroplast membranes through its C-terminal portion. VIPP1 possesses a unique C-terminal tail (Vc) that does not exist in PspA (Fig. 1A), consisting of a stretch of 38 amino acids (Kroll et al., 2001; Aseeva et al., 2004). Vc contains a domain of the α-helical structure that is connected to the PspA-like portion by a random coil spacer of variable length. One Leu and one or two Pro residues (LP or LPP) are always found at the beginning of the random coil region. The α-helix in Vc of most organisms shows higher amino-acid similarity and carries a conserved motif (I/V–EL–LR; Vothknecht et al., 2012). In addition, our preliminary result implicates that Vc faces the surface of VIPP1 complex because it is sensitive to trypsin digest. Consequently, Vc is believed to play important roles in the dynamic behavior of VIPP1, but no additional information has been provided to date. Results show that Vc represents an intrinsically disordered region (IDR) with the ability to regulate the flexibility of association/disassociation of VIPP1 particles. In fact, Vc is necessary to maintain its function against heat stress recovery, suggesting that VIPP1 has acquired its ability to repair photosynthetic membranes. Furthermore, we demonstrate that ectopically expressed VIPP1 enhances tolerance against heat shock stress.

RESULTS

Vc Is Intrinsically Disordered

We first investigated Vc based on in silico prediction programs. PspA and VIPP1 share the position and length of α-helices throughout all amino-acid residues, except for the VIPP1-specific addition of N-terminal transit peptide (TP) and Vc (Fig. 1A). In addition, PSIPRED prediction (Bioinformatics Group, University College London, London, UK) gave us an extremely high probability of Vc as IDR, with many hydrophilic polar residues (Fig. 1B). This IDR property was disrupted at position 225. To ascertain whether Vc represents an IDR or not, circular dichroism (CD) spectra of a synthetic peptide (Fig. 1C; Supplemental Figs. S1 and S2) precisely corresponding to Vc (38 amino acids) were examined. Regular secondary structural elements such as α-helix and β-sheet in globular proteins produced characteristic spectral peaks at 208, 222, and 214 nm, although a large negative peak at approximately 202 nm is characteristic to the coil conformation that dominates in disordered proteins (Receveur-Bréchot et al., 2006). The minimum spectrum of Vc at around 200 nm typically showed the property of IDR (Fig. 1C). The small negative peak at approximately 224 nm possibly corresponds to the region (between 243 and 256 amino acids) that forms, preferably, a short amphipathic α-helix with one hydrophobic face comprising conserved nonpolar residues, opposite to the hydrophilic residues marked in red (Supplemental Fig. S3). The ellipticity at 202 nm was monitored upon increasing the temperature, and was found to increase gradually (Supplemental Fig. S2, A and B). However, the lack of an obvious thermal transition indicated that Vc does not take a prominent secondary structure. In addition, the slight CD spectral change was reversible.

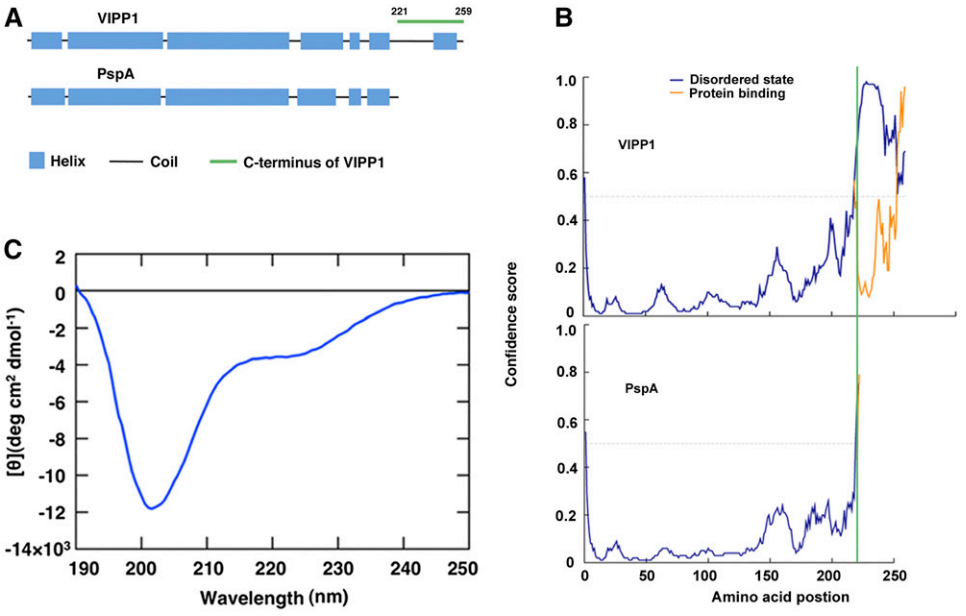

Figure 1. Intrinsically disordered property of Vc. A, Comparison of secondary structures between VIPP1 and PspA predicted by PSIPRED. Blue and black bars, respectively, represent the α-helix and the random coil. A peptide corresponding to Vc (from 221 to 259 amino acids) is marked by a green line. B, Probability plot of IDR in VIPP1 (top) and PspA (bottom) using PSIPRED. The disordered stretch corresponding to Vc is to the right side of the green line. C, CD spectra of 190 to 250 nm at room temperature.

To quantitatively analyze the composition of Vc, the CD spectra were deconvoluted into Helix1, Helix2, Strand1, Strand2, Turns, and Unordered (Supplemental Fig. S2C). The results indicated that the regular helix is only 3.4%, and the bulk of Vc showed a disordered character. Based on these observations, we concluded that VIPP1 is partially disordered at Vc.

Vc Alters VIPP1's Supercomplex Formation

Next, we tested how Vc affects the VIPP1 supercomplex assembly. Structural analysis revealed that VIPP1 assembles into a homooligomeric ring structure (designated hereinafter as functional VIPP1 particle, or FVP) with high molecular mass in vivo and in vitro, which is dependent on α-helix at its N terminus (Aseeva et al., 2004; Otters et al., 2013; Zhang and Sakamoto, 2015). Microscopic observations of protoplasts or guard cells from transgenic lines over-expressing VIPP1-GFP and VIPP1Δc-GFP (lacking Vc) in the wild-type Arabidopsis (*Arabidopsis thaliana*) ecotype Columbia (Col) revealed that the deletion of Vc altered the patterns of VIPP1 supercomplex and induced excessive mutual association of FVP (Fig. 2A). The VIPP1Δc-GFP particles per chloroplast were markedly fewer in *VIPP1Δc-GFP*/Col than in *VIPP1-GFP*/Col (Fig. 2B). Similarly, the average numbers of larger and irregular particles/clumps (>1.5 μm) increased more in *VIPP1Δc-GFP*/Col than in *VIPP1-GFP*/Col (Fig. 2C). To check this result further, total chloroplast proteins purified from these plants were separated by native PAGE followed by second-dimension SDS-PAGE and western blotting (Supplemental Fig. S4). As reported previously, VIPP1 and VIPP1-GFP formed a large complex of >1 MDa whose size is comparable to those in Col (Zhang et al., 2012). VIPP1Δc-GFP also formed a larger complex and co-migrated with endogenous VIPP1. Based on these results, we concluded that Vc deletion leads FVP to self-associate to form larger clumps, thereby Vc negatively controls VIPP1's homooligomeric assembly.

Consistent with the clustering of VIPP1Δc-GFP inside chloroplasts, particle analysis of negatively stained VIPP1Δc expressed in *Escherichia coli* also presented a clustering of FVP when Vc was deleted (Fig. 2, D and E). Observation of VIPP1Δc FVPs using TEM demonstrated that the clusters consisting of two or more particles accounted, respectively, for 17.2% or 18.2% of all FVPs. In contrast, FVPs from VIPP1 were detected as single particles (Fig. 2F). We noted this result was somewhat different from previous observations of FVPs in other organisms (e.g. Liu et al., 2007 in *Chlamydomonas*), in which even native VIPP1 was reported to form rod-like aggregates in vitro. We accounted for the observed discrepancy for the different experimental condition, because P instead of Tris buffer was used in our study. To test this possibility, we replaced buffer by dialysis with Tris buffer and subjected VIPP1 particles to TEM analysis (Supplemental Fig. S5). The result indeed showed that VIPP1 was able to form rods that appeared to consist of FVPs as previously reported. VIPP1Δc also formed rods, but it tended to show highly variable structures like long rods and clustered larger particles, all of which were rarely detectable in our VIPP1 preparation. Given that our result is consistent with those from Otters et al. (2013), we considered that VIPP1Δc aggregates more than VIPP1 in Arabidopsis in vitro. Along with the observation of VIPP1Δc-GFP in vivo, these results demonstrated that Vc acts in preventing clustering and in retaining the flexibility of FVPs.

Excessive Clustering of VIPP1Δc-GFP Constrains Its Dynamics inside Chloroplasts

To assess the effect of Vc deletion on VIPP1 dynamics, hypotonic stress was given to protoplasts isolated from *VIPP1-GFP*/Col or *VIPP1Δc-GFP*/Col, as reported previously in Zhang et al. (2012). We have shown that hypotonic treatment of mesophyll cells, protoplasts, or purified chloroplasts caused VIPP1 to disassemble and to become highly mobile in the areas where stroma is swollen due to the hypotonic stress (examples are shown in Supplemental Videos 1 and 2, and a bright-field still image is shown in Supplemental Fig. S6). Under moderate hypotonic stress (H_2O: buffer is 1:4 [v/v], equivalent to 0.56 Osmol/L), only a few small FVPs in transgenic lines showed movement (Fig. 3A, left panel, indicated by white arrowheads, Supplemental Videos 3 and 4). Upon increasing the hypotonic stress (H_2O: buffer is 1:1 [v/v], equivalent to 0.35 Osmol/L), however, most particles began to move (Fig. 3A, middle panel, indicated by yellow arrowheads, Supplemental Videos 5 and 6). Similar dynamics of VIPP1-GFP particles was also observed with isolated chloroplasts or mesophyll cells of leaves under hypotonic stress conditions (Supplemental Videos 1 and 2). Dynamic movement of VIPP1-GFP is always concomitant with the hypotonic stress, which leads to the observation of swollen chloroplasts (Zhang et al., 2012). Time-lapse fluorescence images of Figure 3B presented tracking observation of moving VIPP1 signals under this condition. No noticeable movement of VIPP1-GFP or VIPP1Δc-GFP particles was detected in protoplast without hypotonic stress (Fig. 3A, right panel, Supplemental Videos 7 and 8). This mobile characteristic of VIPP1Δc-GPF particles suggests that Vc is not necessary for FVP to retain its ability to move, and that it is consistent with the fact that PspA by itself has the capacity to move. Our live-imaging therefore supports our notion that Vc acts to prevent FVP from forming excessive aggregation. We infer that large particles in *VIPP1Δc-GFP*/Col do not respond promptly to membrane stress, which therefore engenders a decreased recovery rate against stress (see below).

Vc Enables PspA to Assemble Like FVP in Chloroplasts

VIPP1Δc segment shows high similarity with bacterial PspA, raising the possibility that the two proteins act redundantly. Our previous study demonstrated

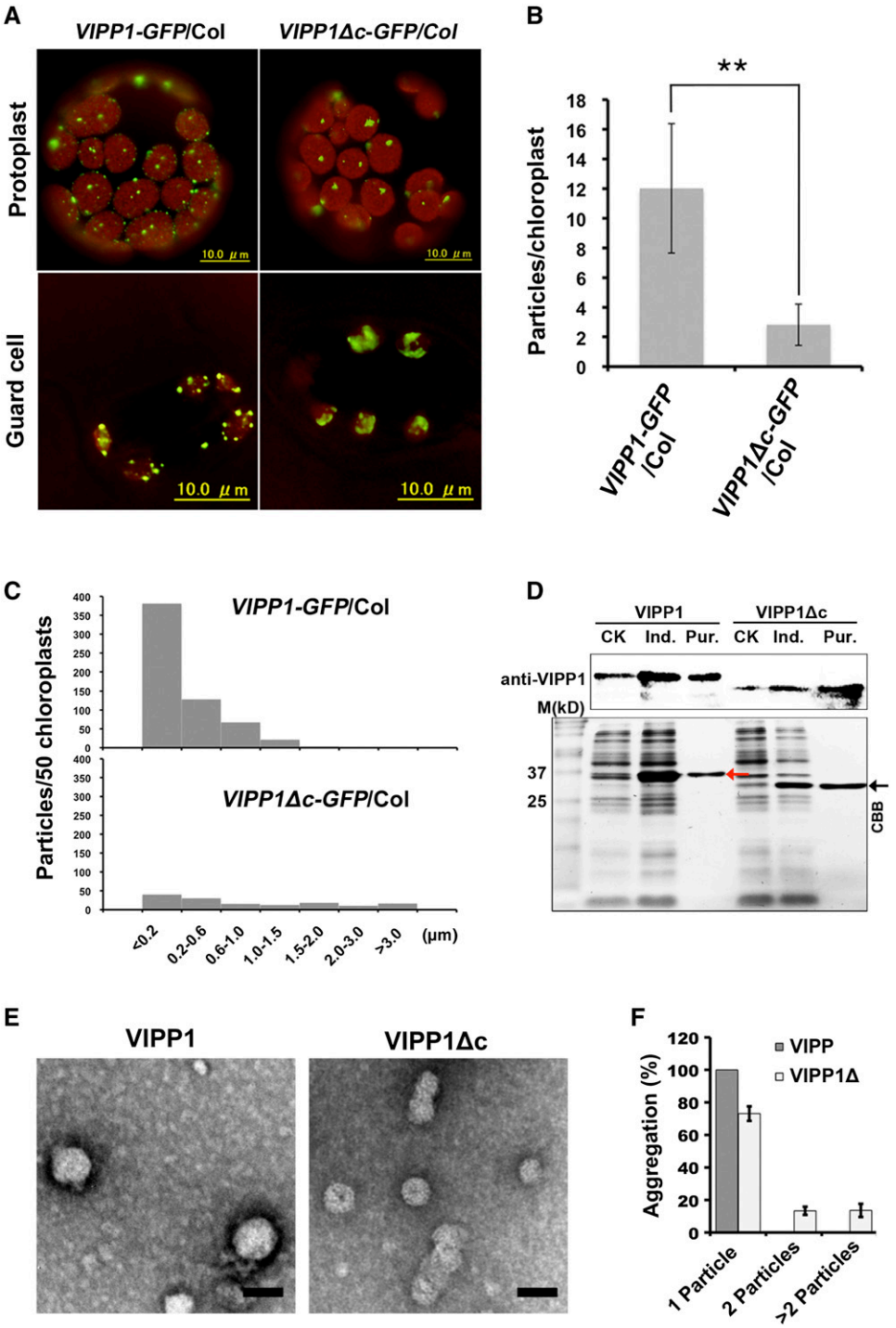

Figure 2. Effects of Vc on the clustering of VIPP1 particle in Arabidopsis. A, Representative mesophyll protoplasts and guard cells of *VIPP1-GFP*/Col (left) and *VIPP1Δc-GFP*/Col (right). Chlorophyll autofluorescence and GFP signals are shown as red and green, respectively. B, Number of GFP particles per chloroplast in protoplasts from *VIPP1-GFP*/Col (left) and *VIPP1Δc-GFP*/Col (right; $n = 50$, $^{**}P < 0.01$). C, Histograms showing the distribution of different sizes of GFP particles (estimated by the maximal diameter of each particle) are shown ($n = 50$). D, Expression and purification of His-tagged VIPP1 and VIPP1Δc fusion proteins in *E. coli*. Red and black arrowheads, respectively, indicate the VIPP1 and VIPP1Δc positions. E, Recombinant VIPP1 and VIPP1Δc expressed and purified from *E. coli* in P buffer were visualized using negative stain and subsequent observation by TEM. Bars = 40 nm. F, Clustering of VIPP1 and VIPP1Δc particles estimated using the number of self-associating particles (single, two, and more than two particles, $n = 30$). CK, extracts from bacterial culture without IPTG; Ind., extracts from bacterial culture supplemented with 0.8 mM IPTG for induction; Pur., VIPP1 (left) or VIPP1Δc (right) fusion proteins purified from IPTG-induced *E. coli* lysates.

that VIPP1 can complement a defective proton-motive force of *pspA* mutation in *E. coli*. Nevertheless, PspA expression has not been tested in Arabidopsis chloroplasts. To test this possibility, two fusion proteins PSPA-GFP or PSPAvc-GFP were over-expressed in Col under the constitutive CaMV *35S* promoter (Fig. 4A). These proteins were expressed as fused to the N-terminal transit peptide derived from VIPP1 (TP_{vip}), so as to deliver them to chloroplasts. Immunoblot analysis of these plants, *PSPA-GFP*/Col and *$PSPA_{VC}$-GFP*/Col, indicated that each fusion protein accumulated comparatively (Supplemental Fig. S7A, proteins loaded on a fresh weight basis). Similar to the case in VIPP1Δc-GFP, PSPA-GFP was detected as larger and irregular particles inside chloroplasts (Fig. 4B). In contrast, PSPAvc-GFP formed smaller particles, similar to those of FVPs observed in *VIPP1-GFP*/Col (Fig. 4B). Addition of Vc enabled PspA to form smaller

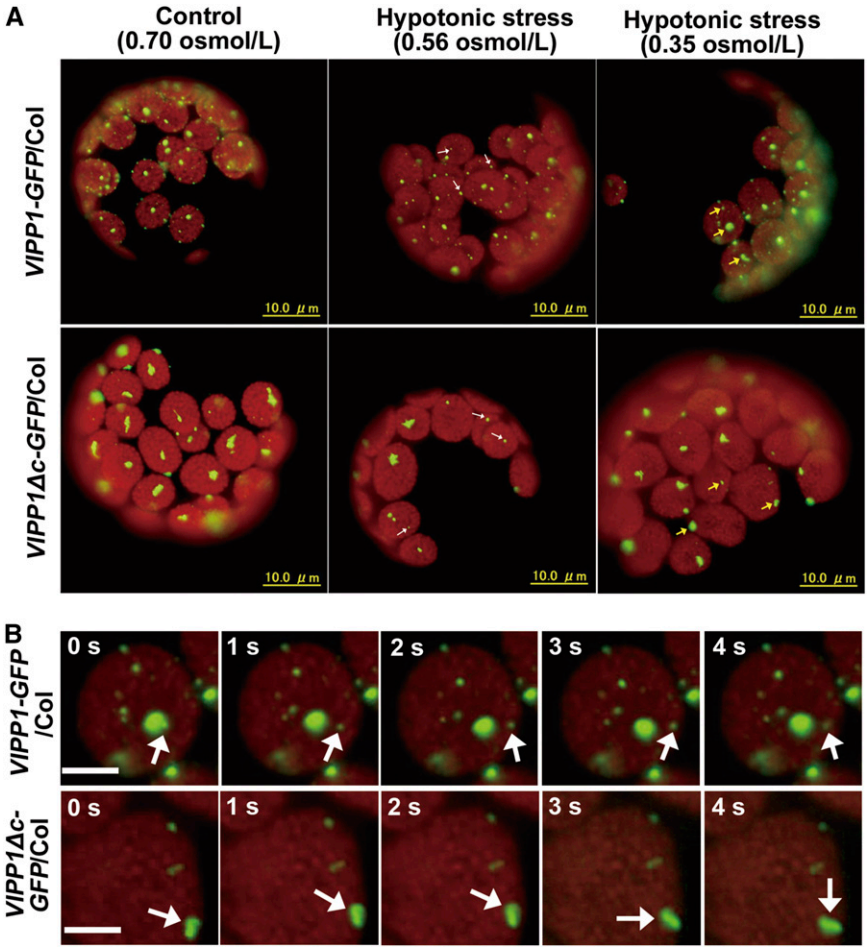

Figure 3. Movement of VIPP1-GFP and VIPP1Δc-GFP particles in chloroplasts after hypotonic stress treatment. A, Intact protoplasts isolated from 3-week-old seedlings of *VIPP1-GFP*/Col (top) and *VIPP1*Δ*c-GFP*/Col (bottom) were given hypotonic stress by treating them with 20% or 50% diluted suspension buffer (left and middle panels, respectively), and were recorded by microscopic observation as time-lapse images. Control protoplasts without hypotonic stress are shown on the right. Observations were conducted at least 5 min after osmotic treatment. Arrowheads indicate VIPP1-GFP particles that showed movement. Movies corresponding to each panel are shown as Supplemental Videos 3–8. B, Time-lapse fluorescence images of the representative chloroplasts suffering from hypotonic stress at 50% dilution. Bars = 5 μm. Five images of the representative chloroplasts from *VIPP1-GFP*/Col (top) and *VIPP1*Δ*c-GFP*/Col (bottom) are shown. Arrows indicate typical particles showing movement.

clumps, followed by an increased number of particles per chloroplast (Fig. 4, C and D). Consequently, these results demonstrated that Vc negatively affects both VIPP1 and PspA clustering status in vivo.

We next performed complementation experiments of *vipp1-ko* with PSPA-GFP or PSPAvc-GFP (Fig. 4E). Immunoblot analysis of these transgenic lines (*PSPA-GFP/vipp-ko* and *PSPA*$_{VC}$*-GFP/vipp1-kko*) ensured comparable expression levels between the two lines (Supplemental Fig. S7B). The results showed that the lack of VIPP1 causes a severe defect in chloroplast biogenesis; *vipp1-ko* (complete knock-out and no VIPP1 is detectable) dies at the seedling stage with albino-like phenotype. Despite the structural similarity in the complex formation described above, neither PSPA-GFP nor PSPAvc-GFP complemented the seedling lethality of *vipp1-ko* (Fig. 4F). No functional exchangeability between PspA and VIPP1 has been reported in *Synechocystis* (Westphal et al., 2001; DeLisa et al., 2004). Together, our results demonstrated that the N-terminal PspA-like sequences of VIPP1 include important information that is useful to distinguish VIPP1 from PspA, most likely because of a different binding ability to the partner proteins. Nevertheless, we infer that intrinsically disordered Vc acts in both PspA and VIPP1 to give its complex formation and structural flexibility, which is expected to be related to the membrane repair capacity.

Vc Is Necessary for Membrane Protection against Heat Shock Recovery

We assessed whether VIPP1Δc-GFP can complement the lethality of *vipp1-ko*. We generated transgenic lines that expressed VIPP1-GFP or VIPP1Δc-GFP by *VIPP1*'s own promoter under a *vipp1-ko* background (Fig. 5A). These two lines, *Pv-VIPP1-GFP/vipp1-ko* and *Pv-VIPP1*Δ*c-GFP/vipp1-ko*, grew normally and presented chloroplast morphologies that were indistinguishable from those in Col (Fig. 5B), demonstrating that Vc is dispensable. We confirmed that both transgenic lines accumulated VIPP1-GFP or VIPP1Δc-GFP to a level similar to endogenous VIPP1 in Col (Fig. 5C). It is noteworthy that FVPs visualized by VIPP1-GFP and VIPP1Δc-GFP were distinguishable, as was observed by over-expression (Fig. 2): VIPP1Δc-GFP showed larger clumps whereas VIPP1-GFP FNPs were smaller and round (Fig. 5D), implicating that the observed difference in FNP structures do not influence plant growth under normal conditions.

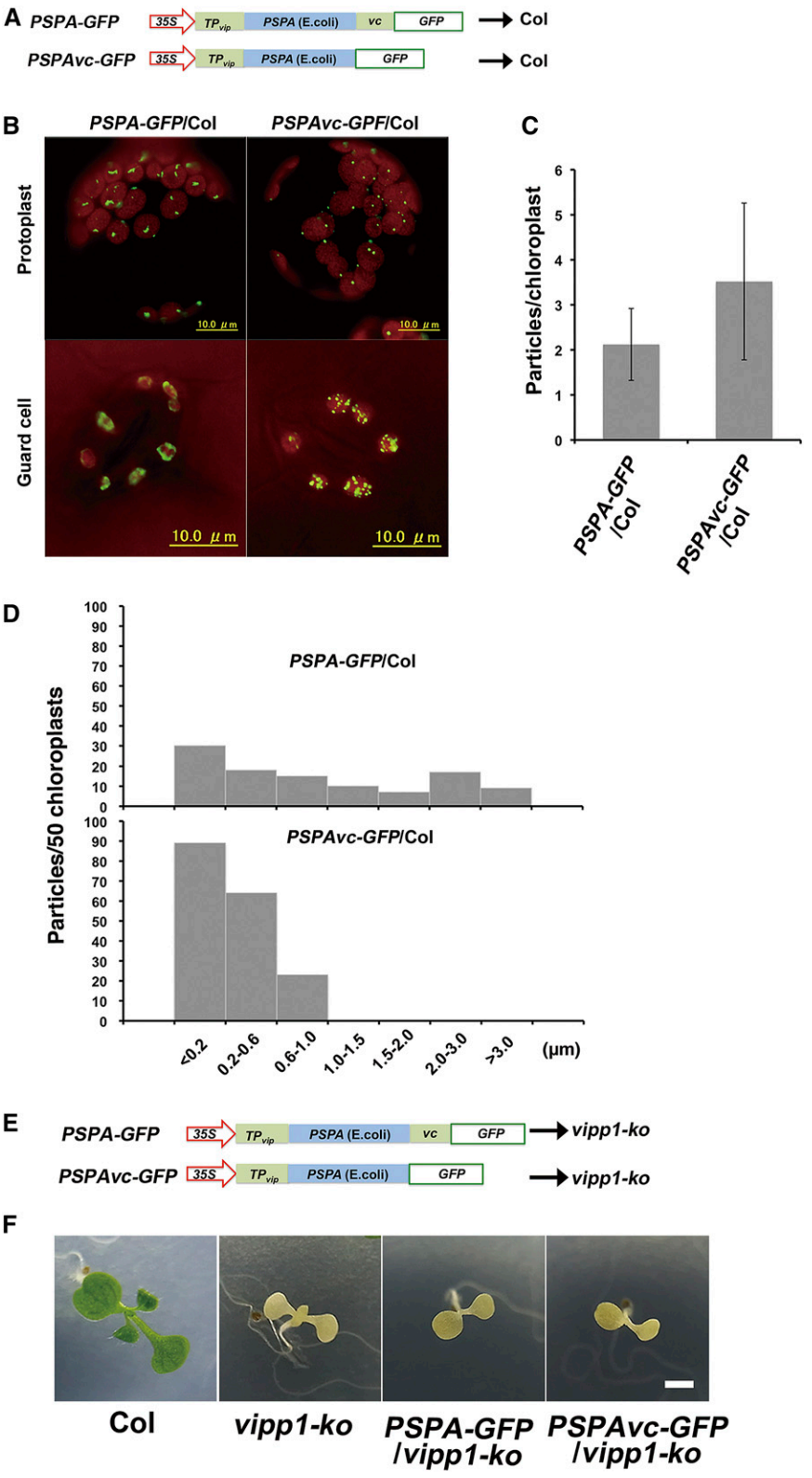

Figure 4. Effects of Vc on the PspA particle in Arabidopsis and complementation of *vipp1-ko* mutant with *PspA-GFP* and *PSPAvc-GFP*. A, Schematic illustration of *PSPA-GFP* and *PSPAvc-GFP* constructs used for transformation into Col. TP_{vip} indicated the transit peptide of Arabidopsis VIPP1. B, Representative mesophyll protoplasts and guard cells of *PSPA-GFP*/Col (left) and *PSPAvc-GFP*/Col (right). Chlorophyll autofluorescence and GFP signals are depicted respectively as red and green. C, Numbers of GFP particles per chloroplast in protoplasts of *PSPA-GFP*/Col (left) and *PSPAvc-GFP*/Col (right; $n = 50$). D, Histograms showing the distribution of different sizes of GFP particles (estimated by the maximal diameter of each particle; $n = 50$). E, Schematic illustration of *PSPA-GFP* and *PSPAvc-GFP* constructs used for transforming *vipp1-ko*. F, Phenotypes of 7-d-old seedlings grown on MS agar medium. Bar = 3 mm.

We assumed that Vc gives VIPP1 the capacity for flexible formation of supercomplexes under stress conditions, and that the presence or absence of Vc may affect response to stress conditions leading to membrane damage. Therefore, *Pv-VIPP1-GFP/vipp1-ko* and *Pv-VIPP1Δc-GFP/vipp1-ko* were characterized further for their photosynthetic activities under various stress conditions. Given that bacterial PspA is highly

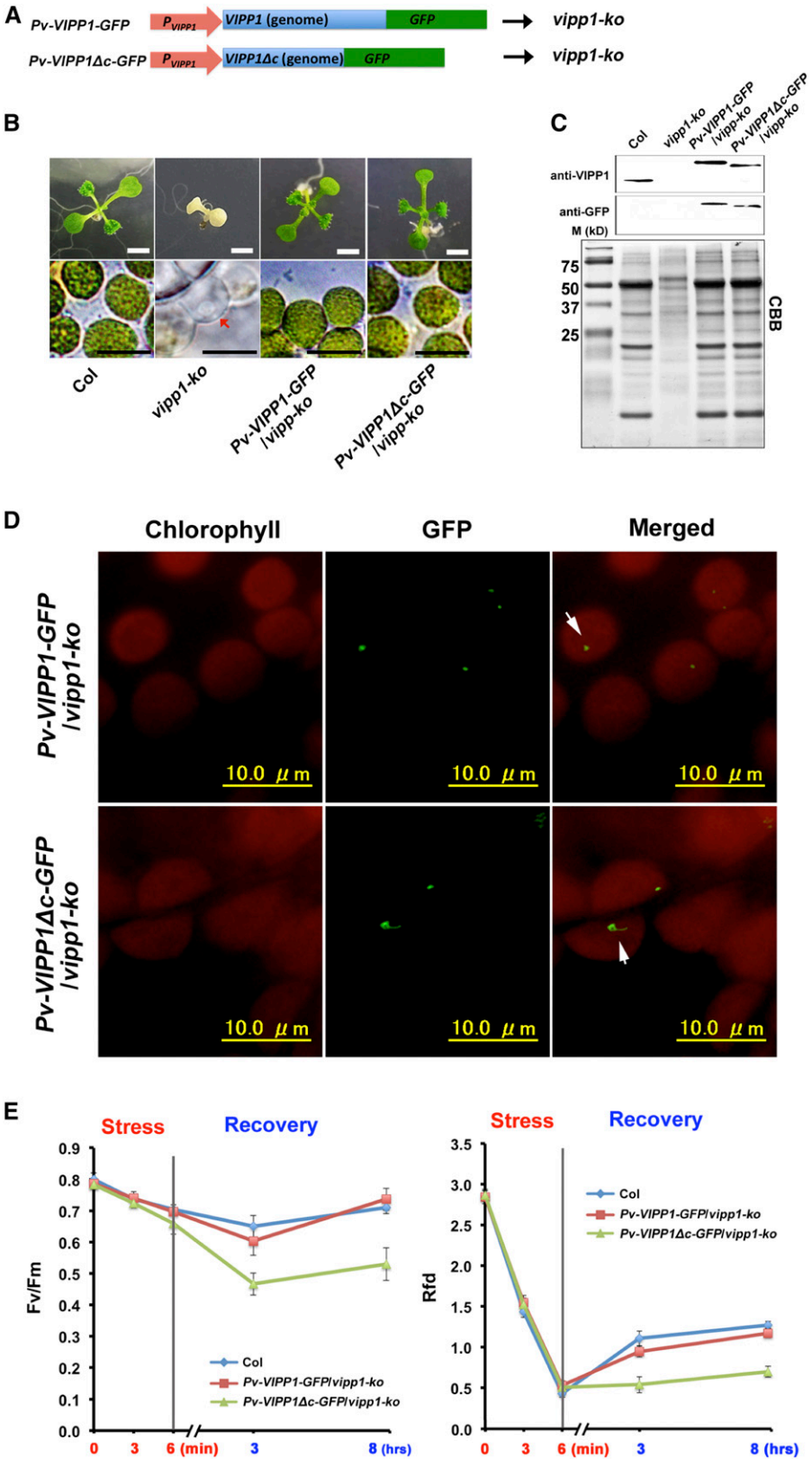

Figure 5. Complementation of the *vipp1* knockout mutant (*vipp-ko*) with *Pv-VIPP1-GFP* or *Pv-VIPP1Δc-GFP*, and characterization of heat shock tolerance. A, Schematic illustration of two constructs used for complementation: *Pv-VIPP1-GFP* and *Pv-VIPP1Δc-GFP*. B, Photographs of 10-d-old seedlings from different lines (upper panels, bar = 3 mm) and chloroplast/plastid observed directly using bright-light microscopy (lower panels; bars = 10 μm). Colorless plastid of *vipp-ko* mutant is indicated by a red arrowhead. C, Accumulation of VIPP1-GFP and VIPP1Δc-GFP confirmed by western blots. D, In situ observation of VIPP1-GFP and VIPP1Δc-GFP particles in the leaves of *Pv-VIPP1-GFP/vipp1-ko* and *Pv-VIPP1Δc-GFP/vipp1-ko*, respectively. E, The Fv/Fm (left) and Rfd (right) of detached leaves from 3-week-old seedlings of Col (blue), *Pv-VIPP1-GFP/vipp1-ko* (red), and *Pv-VIPP1Δc-GFP/vipp1-ko* (green) that were treated with a heat shock at 45°C for 6 min.

induced by extreme heat shock and that it acts in maintaining cytoplasmic membrane integrity, VIPP1 is likely to protect chloroplast membranes against heat shock. To test this possibility, detached leaves from these transgenic lines were subjected to heat shock stress (45°C for 6 min followed by recovery period for

8 h) and measured chloroplast activity based on chlorophyll fluorescence parameters. As a reference, we measured the relative fluorescence decline (Rfd) and photosystem II photochemical efficiency (Fv/Fm). Rfd, as a plant vitality index, is correlated to the potential photosynthetic net CO_2 fixation rate of the Calvin cycle (Tuba et al., 1994; Lichtenthaler and Miehé, 1997). Results show that the lack of Vc in *Pv-VIPP1Δc-GFP/vipp1-ko* markedly disturbs chloroplast function at the recovery stage of heat shock stress (45°C for 6 min). Recovery of Rfd and Fv/Fm after exposure to heat stress suggested that repair processes were activated in these plants. However, Fv/Fm and Rfd decreased dramatically in *Pv-VIPP1Δc-GFP/vipp1-ko*, especially at the recovery stage (Fig. 5E). The weak recovery of *Pv-VIPP1Δc-GFP/vipp1-ko* reflected that Vc plays a crucially important role in chloroplast membrane repair under heat stress conditions.

VIPP1 Overexpression Improves Recovery from Heat Shock

The possible involvement of Vc in membrane repair prompted us further to examine whether VIPP1 overexpression protects chloroplasts against heat shock and recovery. In this attempt, VIPP1 was expressed constitutively by a CaMV *35S* promoter in a Col background (*VIPP1*/Col). Based on immunoblots, we verified that *VIPP1*/Col accumulated high levels of VIPP1 (>10-fold) compared to Col; Fig. 6, A and B). Resolution of chloroplast proteins in a native PAGE gel followed by second-dimension SDS-PAGE revealed that overexpressed VIPP1 in *VIPP1*/Col formed high M_r supercomplexes, which are similar to those of endogenous VIPP1 (Fig. 6C). As expected, detached leaves from *VIPP1*/Col lines showed faster recovery of Rfd and Fv/Fm after heat treatment and recovery than those of Col, suggesting that VIPP1 indeed acts in protecting chloroplast membranes (Fig. 6D). Based on these results, we concluded that ectopic expression of VIPP1 enhances tolerance of Arabidopsis against heat shock stress.

DISCUSSION

VIPP1 Is Partially Disordered with Its Unique C Terminus

PspA, a versatile membrane-repair system conserved between bacteria and chloroplasts, is necessary to maintain membrane potential against various membrane stresses. During evolution of photosynthetic organisms, however, the PspA ortholog (VIPP1) seems to have acquired an additional C-terminal tail, which engenders its extraordinary capacity to repair photosynthetic membranes. For this study, we specifically examined this additional C-terminal tail (Vc) in Arabidopsis, and demonstrated the following: (1) Vc is partially disordered; (2) Vc acts in promoting flexible mobility against stress by preventing self-association of FVPs; and (3) the elevated expression of VIPP1 improves the tolerance of chloroplasts against heat shock. Dynamic movement of VIPP1 upon stress is a prerequisite for such tolerance, as is true also of PspA in *E. coli*. Based on these observations, we inferred that Vc is dispensable but important for protecting photosynthetic membranes against stress. Given that intrinsically disordered proteins (IDPs) and IDRs are detected dominantly in eukaryotes, Vc presents an interesting example of protein evolution and adaptation to different environments. How this C-terminal tail emerged during evolution remains unclear because Vc has no apparent homology to known proteins.

Intrinsic disorder is assumed to provide several functional advantages such as increased interaction surface area, structural plasticity to interact with multiple targets, and the ability to fold upon binding. In fact, VIPP1 reportedly interacts with chaperone-like proteins Hsp70, CDJ2, and CGE1 (Liu et al., 2005; 2007; Gao et al., 2015), Hsp90C (Heide et al., 2009), and Albino3.2 (Göhre et al., 2006). Interaction with these chaperones is apparently regulated by ATP. In addition, VIPP1 is reportedly associated with TIC-TOC complexes (Jouhet and Gray, 2009), inner envelopes as well as thylakoid membranes of chloroplasts (Li et al., 1994), cytoplasmic and thylakoid membranes of cyanobacteria (Srivastava et al., 2005; Fuhrmann et al., 2009), and lipids of *E. coli* (Otters et al., 2013). All these interactions/associations confirm the important role of VIPP1 as a natively disordered protein. Another general feature of IDPs is susceptibility to proteolytic degradation in vitro (Sun et al., 2013). The fact that Vc was digested more easily by trypsin than the N-terminal domain reflects this feature (Aseeva et al., 2004). All circumstances are consistent with the idea that VIPP1 represents a partially disordered protein.

Vc Regulates the Flexibility of FVP Association

VIPP1 was assigned as a membrane-attached protein since its initial discovery in pea chloroplast (Li et al., 1994): approximately 80% was localized on chloroplast envelope; the remainder was localized in the thylakoid membrane (Kroll et al., 2001). To exert its function, VIPP1 has been shown to form homo-oligomeric supercomplex as a functional unit (FVP) on the membranes. Reportedly, the N terminus, rather than the C terminus of VIPP1, is necessary for oligomerization in vitro (Otters et al., 2013), which might be potentially further clarified on the base of crystal structure study of $PspA_{1-144}$ (Osadnik et al., 2015). This is consistent with our data showing that Vc does not affect FVP formation directly. Nevertheless, previous negative stain and particle analysis revealed the important role of FVPs. Upon hypotonic stress, FVP clusters dissociate and appear to repair the damaged membranes, although molecular details related to this repair mechanism remain unclear. Future analysis of VIPP1 movement against hypotonic stress is expected to facilitate our understanding of the factors involved. It is noteworthy that FVPs observed as VIPP1-GFP

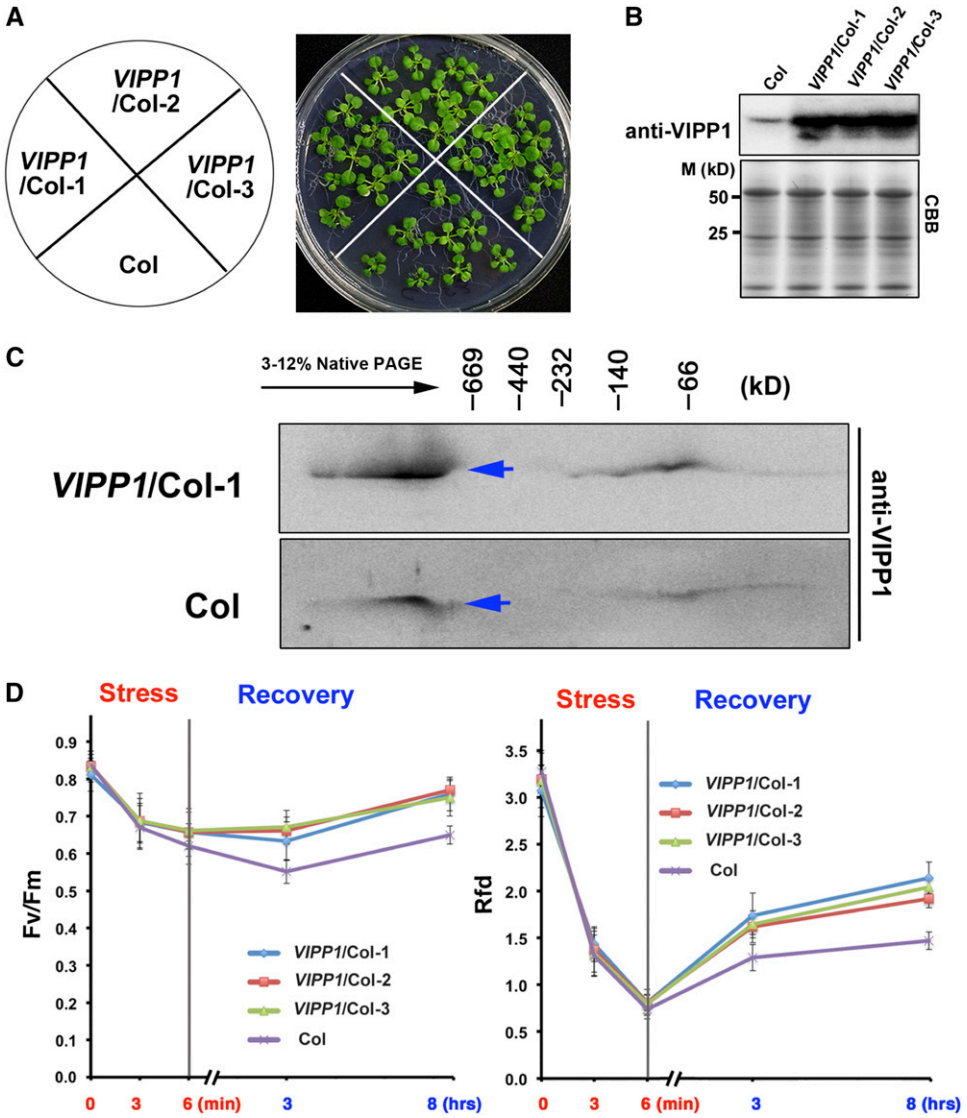

Figure 6. Heat shock tolerance of *VIPP1*/Col. A, The phenotype of 17-d-old seedlings of Col and three different transgenic lines (1, 2, and 3) of *VIPP1*/Col. B, The protein level of VIPP1 in Col and transgenic lines. C, Analysis of VIPP1 supercomplexes of Col and *VIPP1*/Col-1 with native PAGE. Blue arrows indicate the supercomplexes of VIPP1. D, The decrease and recovery of Fv/Fm (left) and Rfd (right) of detached leaves from Col (purple) and three *VIPP1*/Col lines (blue, red, and green) that were treated with a heat shock at 45°C for 6 min.

in vivo or negatively stained VIPP1 particles in vitro became more clustered when Vc was deleted (Fig. 2). Irregular clustering of VIPP1Δc appeared to result from the random assembly of FVPs. These results imply that Vc is likely faced to the surface area of FVPs to prevent clustering. Consistent with this accessory role, VIPP1Δc-GFP complemented *vipp1-ko* (Fig. 5). However, we cannot rule out the possibility that Vc deletion engenders a conformational change of single FVP because VIPP1Δc particles exhibited reduced size in negative stain (Fig. 1).

VIPP1 Complex and Lipid Binding

Otters et al. (2013) found that a recombinant VIPP1 purified from *E. coli* binds lipids tightly enough to enable co-purification even after several isolation procedure steps. They also reported that the deletion of C terminus (outermost 40 amino acids) reduced lipid association along with more FVP stacking. Although circumstantial, the provided evidence thus implies that Vc may influence lipid biding: the hydrophobic face on one side of amphipathic α-helix of Vc possibly allows it to bind with lipids. Recently, membrane fusion mediated by VIPP1 in *Synechocystis* has been reported in vitro (Hennig et al., 2015). This in vitro work showed that FVPs preferentially bind to anionic lipids like sulfoquinovosyldiacyl glycerol and phosphatidyl glycerol. It is interesting to examine whether VIPP1 also binds to specific lipids in vivo and if Vc has any role in assisting lipid binding. Similarly to VIPP1, the C terminus of phosphatase and tensin homolog in humans is IDR. It is reported to regulate phosphatase and tensin homolog membrane association, stability, and activity (Vazquez et al., 2000; Ross and Gericke, 2009). An alternative possibility is that VIPP1 behaves similarly to an apolipoprotein A-I that holds lipids. Apolipoprotein A-I is an amphipathic protein that can interconvert between a soluble lipid-free state and a lipid-bound

form, with the lipid-free form able to self-associate into the different particle sizes. It is particularly interesting that lipid binding is regulated by its random coiled C terminus (Ajees et al., 2006).

VIPP1 as a Protein for Membrane Protection against Stress

Our supposition that VIPP1 acts in protecting envelopes is based on the swollen chloroplast phenotype observed in *vipp1-kd* and *vipp-ko*, which results from compromised response to the osmotic or hypotonic stress of chloroplasts. Reportedly, chloroplast envelopes were shown to be one of the sites for damage against abiotic stress. For example, a lesion occurs in the chloroplast envelope membrane at a temperature between 53°C and 57°C, depending on leaf conditions and heating rate upon the plant. As a result, sudden loss of water from the chloroplast was detectable (McCain et al., 1989). When maize plants were subjected to both drought and heat stresses, chloroplasts were observed to be swollen and envelope membrane was interrupted (Dekov et al., 2000). Low temperate also seems to induce damage to the chloroplast envelope. Ma et al. (1990) found the envelopes of chloroplasts were disrupted in many places when mung bean (*Vigna radiata*) suffered from chilling treatment. Tanaka (2007) compared the structure of chloroplasts in summer and winter needles of *Taxus cuspidata* and found that most of the chloroplasts were swollen, which implied that envelope membrane was damaged by the low temperature. Consistent with these results, damaged envelopes were observed in *vipp1-kd* leaves (Supplemental Fig. S8).

In this study, we demonstrated that over-expression of VIPP1 prevents the Arabidopsis plant from being damaged by heat shock. Moreover, we recently found that VIPP1 over-expression transcomplements growth defects in the mutant other than *vipp1* (Zhang et al., 2016), together corroborating our previous hypothesis that VIPP1 plays a role in membrane protection. How does VIPP1 exert its function in membrane protection? Although the possible involvement in vesicle transfer, lipid transfer, and membrane fusion has been proposed, it still needs further investigation. Another question is what energy drives the dynamic behavior of FVPs evidenced by our imaging analysis. It was reported that assembly and disassembly of FVPs was regulated by Hsp70B-CDJ2-CGE1 complex in an ATP-dependent manner (Liu et al., 2007). The flexibility of FVPs association was regarded as important process for the membrane repair. It is possible that, around the membrane damage site, stronger interaction between HSP70 and VIPP1 induces the release of lipids from the hydrophobic surface of VIPP1, with concomitant assembly of FVPs. Just like its ancestor PspA of *E. coli*, the dynamics of VIPP1 is involved in membrane repair (Zhang et al., 2012). Excessive clustering of VIPP1Δc particles severely constrains its dynamics, giving rise to its susceptibility to heat shock. In contrast, most wild-type FVPs respond to hypotonic stress and display dynamic movement (Supplemental Videos 1 and 3). Most recently, membrane fusion has been suggested to be triggered by IM30/VIPP1 in cyanobacteria (Hennig et al., 2015). McDonald et al. (2015) also proposed the protective function of PspA and VIPP1 high-order oligomers in alleviating membrane-stored curvature elastic stress by amphipathic helix insertion. Both of them strongly supported our notion that VIPP1 plays a role in maintaining membrane integrity in chloroplasts.

CONCLUSION

It is increasingly clear that IDPs and IDRs are vital to many biological processes, particularly in stress response (Sun et al., 2013). For example, LEA (early response to dehydration) proteins, a plant protein family with the largest number of known IDPs, can protect membranes against drying and chilling (Tolleter et al., 2010). In this study, we demonstrated that VIPP1 as an IDP plays a role in chloroplast membrane protection stress. Considering that the envelope is prone to heat shock, this result is consistent with our previous hypothesis that VIPP1 is responsible for envelope maintenance (Zhang et al., 2012; Zhang and Sakamoto, 2013; 2015). Overall, our data support our notion that VIPP1 is important for protecting photosynthetic membranes, which is supported by the acquisition of Vc.

MATERIALS AND METHODS

Plant Materials, Generation of Transgenic Lines, and Growth Conditions

Arabidopsis (*Arabidopsis thaliana*) ecotype Columbia (Col-0) was used as the wild type in this study. *vipp1-ko and VIPP1-GFP*/Col were reported previously in Zhang et al. (2012). The chimeric constructs *VIPP1Δc-GFP*, *PSPA-GFP*, and *PSPAvc-GFP* were created using an In-Fusion cloning kit (Clontech, Mountain View, CA). In brief, two types of linearized vector (type A: *35S-VIPP1* signal peptide sequence...-*GFP*; type B: *35S-VIPP1* signal peptide sequence…-*Vc-GFP*; deleted sequences are denoted as three dots) were generated by PCR with pGreen0029-VIPP1-GFP as a template. To produce *VIPP1Δc-GFP*, a PCR fragment corresponding to *VIPP1Δc* was In-Fusion cloned into the type-A linearized vector. To produce *PSPA-GFP* or *PSPAvc-GFP*, a *PSPA* fragment was amplified, respectively, from pEC1-PSPA, and In-Fusion cloned into the type-A and type-B linearized vectors. All these genes were placed under the control of the CaMV *35S* promoter. To make *Pv-VIPP1-GFP* and *Pv-VIPP1Δc-GFP*, a genomic sequence corresponding to *VIPP1* and *VIPP1Δc* together with their putative promoter region (670 bp upstream of the initiation codon) were amplified from Col total DNA. These two fragments were In-Fusion cloned into the linearized pGreen0029-VIPP1-GFP without *35S-VIPP1* to replace the fragment corresponding to *35S-VIPP1* with *Pv-VIPP1* or with *Pv-VIPP1Δc*. The resulting plasmids were transformed using *Agrobacterium*-mediated transformation into the plant that is heterozygous for *vipp1* (*VIPP1/vipp1*). Transgenic plants homozygous for the transgenes, *VIPP1Δc-GFP*/Col, *PSPA-GFP*/Col, *PSPAvc-GFP*/Col, *PSPA-GFP/vipp1-ko*, *PSPAvc-GFP/vipp1-ko*, *Pv-VIPP1-GFP/vipp1-ko*, and *Pv-VIPP1Δc-GFP/vipp1-ko*, were selected from the F3 generation. Surface-sterilized seeds were sown onto 0.7% Murashige and Skoog (MS) agar plates supplemented with 1.5% (w/v) Suc. Plants were maintained under light (approximately 70 μmol m^{-2} s^{-1}) with 12 h/12 h light/dark cycles at a constant temperature of 22°C. After 2-week growth on MS medium, the seedlings were transferred to soil.

Protein Secondary Structure Prediction and Circular Dichroism Spectrum

Prediction of an intrinsically disordered region was conducted using PSIPRED (http://bioinf.cs.ucl.ac.uk/psipred) software (Ward et al., 2004). For circular dichroism (CD) spectrum analysis, a peptide corresponding to Vc (38 amino acids) was synthesized commercially (SCRUM, Tokyo, Japan). The CD spectrum of the peptide (0.27 mg/mL in water) was measured using a CD spectropolarimeter (J-725; Jasco, Oklahoma, OK) with a quartz cell. The sample temperature was maintained at 20°C using a Peltier temperature controller (PYC-347WI; Jasco). The secondary structure composition of Vc was predicted based on the CD spectra from 190 to 240 nm using the on-line Circular Dichroism Analysis, DichroWeb (http://dichroweb.cryst.bbk.ac.uk; Whitmore and Wallace, 2008). The algorithm used was Contin-LL (Provencher and Glöckner, 1981; van Stokkum et al., 1990) and the reference database was SMP180 (Abdul-Gader et al., 2011).

Protoplast Isolation and Microscopic Observation

Protoplasts were isolated from fully expanded leaves of *VIPP1*Δ*c-GFP*/Col, *VIPP1-GFP*/Col, *PSPA-GFP*/Col, and *PSPAvc-GFP*/Col as described in a previous report (Zhang et al., 2012). Protoplasts were observed under a fluorescence microscope (BX51; Olympus, Melville, NY). Different filter sets (U-MNIBA2 for green/GFP, U-MWIG2 for red/chlorophyll, U-MWIB2 for both) were selected to detect signals from GFP and chlorophyll autofluorescence.

Protein Expression and Negative Staining

VIPP1 cDNA fragments (without sequences corresponding to the transit peptide, N-terminal 71 amino acid) or *VIPP1*Δc cDNA (without sequences corresponding to Vc) were amplified from pGreen0029-*VIPP1-GFP* by PCR, and were subsequently cloned into the expression vector pCRT7/NT-TOPO (Invitrogen, Carlsbad, CA) N-terminally to a His_6 tag. Expression of the recombinant proteins was induced in an *Escherichia coli* BL21(DE3)lysS strain by adding 0.6 mM IPTG (isopropyl-1-thio-β-D-galactopyranoside) for 3 h at 27°C. Cells were harvested by centrifugation and were disrupted by sonication (Tomy Seiko, Tokyo, Japan). His_6-tagged VIPP1 or VIPP1Δc proteins were purified using HiTrap Chelating HP (GE Healthcare, Washington, NY) in accordance with the manufacturer's instructions. His_6-tagged VIPP1 or VIPP1Δc proteins were expressed and purified from an *E. coli* BL21(DE3)lysS strain. For electron microscopic observation, purified proteins were placed onto a carbon-coated grid hydrophilized by the charge glow. Protein supercomplexes were negatively strained with 2% (w/v) uranyl acetate and rinsed briefly with a drop of water, and then air-dried. Prepared specimens were examined using a transmission electron microscope (H-7650; Hitachi, Tokyo, Japan) and then photographed as digital images.

Motility Assay of VIPP1-GFP and VIPP1Δc-GFP Particles

Hypotonic stress was given to these protoplasts by adding a different volume of distilled water into the wash buffer (154 mM NaCl, 125 mM $CaCl_2$, 5 mM KCl, 2 mM MES, at pH 5.7). For moderate hypotonic stress (20%), 0.8 volume of wash buffer was mixed with 0.2 volume of distilled water (equivalent to 0.56 Osmol/L). For high hypotonic stress (50%), the same volume of distilled water was mixed with the same volume of wash buffer (equivalent to 0.35 Osmol/L). Samples were mounted on a slide on an upright microscope (model no. BX51; Olympus) with a 100× oil objective. A filter set (excitation 480 nm, emission 510 nm, model no. U-MWIB2; Olympus) was selected for detecting signals from both GFP and chlorophyll autofluorescence. Photographs were taken using a microscope-mounted video imaging system that consisted of a cooled CCD camera (model no. DP70; Olympus) operated using the DP controller (Olympus) software package. Real-time movies of VIPP1-GFP and VIPP1Δc-GFP dynamics were captured from 5 min after adding distilled water.

Protein Extraction, SDS-PAGE, and Immunoblot Analysis

Equal fresh weights of Arabidopsis leaves were ground with SHS buffer (0.4 M Suc, 10 mM NaCl, 2 mM $MgCl_2$, and 50 mM HEPES) supplemented with 1 mM Cocktail proteinase inhibitor (Roche, Indianapolis, IN). The homogenate was mixed with the same volume 2 × SDS loading buffer (125 mM Tris-Cl pH 6.8, 2% [w/v] SDS, 5% [v/v] glycerol, 5% [v/v] 2-mercaptoethanol, and 0.05% [w/v] bromophenol blue). An equal volume of solution was loaded into SDS-PAGE. Immunoblot analysis was performed as described in an earlier report (Zhang et al., 2012).

Heat Shock and Chlorophyll Fluorescence

To carry out heat shock, detached leaves of 3-week-old Arabidopsis were treated at 45°C for 6 min, followed by 8-h recovery under normal growth conditions (22°C). Chlorophyll fluorescence parameters of two kinds, fluorescence ratio decline (*Rfd*) and photosystem II maximum photosynthesis efficiency (*Fv/Fm*), were recorded using the FluorCam 700MF (Photon Systems Instruments, Brno, Czech Republic) at the different time points. Three biological replicates were performed. The Rfd value, which indicates the potential photosynthetic activity of leaves, was calculated as the ratio of fluorescence decrease (F_d) from the maximum, caused by the saturating light pulse, to the steady state (*Fs*) (*Rfd* = *Fd*/*Fs*; Lichtenthaler and Rinderle, 1988).

Native PAGE, Two-Dimensional SDS-PAGE, and Western Blotting

Chloroplast proteins isolated from Arabidopsis were treated with 1% DM (n-dodecyl-β-maltoside) supplemented with 1 mM Cocktail proteinase inhibitor (Roche) for 15 min on ice. Samples were loaded onto 3–12% acrylamide gradient gels. The electrophoresis was performed at 4°C. For two-dimensional analysis, excised native-PAGE lanes were incubated in SDS sample buffer (125 mM Tris-Cl pH 6.8, 2% [w/v] SDS, 5% [v/v] glycerol, 5% [v/v] 2-mercaptoethanol, and 0.05% [w/v] bromophenol blue) for 1.0 h, and layered onto 15% SDS polyacrylamide gels containing 8-M urea. Immunoblotting was conducted as described in Zhang et al., (2012).

Accession Numbers

Sequence data of VIPP1 can be found in the Arabidopsis Genome Initiative database under accession number At1g65260.1. Sequence information of PspA can be found in GenBank under accession number U00096.2.

Supplemental Materials

The following supplemental materials are available.

Supplemental Figure S1. SDS-PAGE of synthesized Vc (38 amino acids).

Supplemental Figure S2. CD analysis of the synthesized Vc.

Supplemental Figure S3. Helical wheel projection of Vc.

Supplemental Figure S4.. Over-expression of VIPP1-GFP and VIPP1Δc-GFP in Arabidopsis.

Supplemental Figure S5. Negative stain and TEM observation of VIPP1 and VIPP1Δc particles in Tris buffer.

Supplemental Figure S6. Bright-field still image of the chloroplasts shown in Supplemental Video S2.

Supplemental Figure S7. Immunoblot detection of PSPA-GFP and PSPAvc-GFP in *PSPA-GFP*/Col, *PSPAvc-GFP*/Col, *PSPA-GFP*/*vipp1-ko*, and *PSPAvc-GFP*/*vipp1-ko*.

Supplemental Figure S8. Broken chloroplast/plastids of *vipp1* mutants under TEM.

Supplemental Video S1. VIPP1-GFP particles showing movement when chloroplasts isolated from *VIPP1-GFP*/Col underwent 20% hypotonic stress (equivalent to 0.56 Osmol/L).

Supplemental Video S2. VIPP1-GFP particles showing movement when leaf tissue from *VIPP1-GFP*/Col was infiltrated with water.

Supplemental Video S3. Small VIPP1-GFP particles began to move when the mesophyll protoplast of *VIPP1-GFP*/Col underwent 20% hypotonic stress (equivalent to 0.56 Osmol/L).

Supplemental Video S4. Several small VIPP1Δc-GFP particles began to move when the mesophyll protoplast of *VIPP1*Δ*c-GFP*/Col underwent 20% hypotonic stress (equivalent to 0.56 Osmol/L).

Supplemental Video S5. Some slightly larger VIPP1-GFP particles of *VIPP1-GFP*/Col start moving in the chloroplast of mesophyll protoplast in the condition of 50% hypotonic stress (equivalent to 0.35 Osmol/L).

Supplemental Video S6. Some slightly larger VIPP1Δc-GFP particles of *VIPP1Δc-GFP*/Col start moving in the chloroplast of mesophyll protoplast in the condition of 50% hypotonic stress (equivalent to 0.35 Osmol/L).

Supplemental Video S7. VIPP1-GFP remained static in the chloroplast of mesophyll protoplast without hypotonic stress (equivalent to 0.70 Osmol/L).

Supplemental Video S8. No movement was observed with VIPP1Δc-GFP particles in the chloroplast of mesophyll protoplast without hypotonic stress (equivalent to 0.70 Osmol/L).

ACKNOWLEDGMENTS

We thank Professor Ute C. Vothknecht for providing the antibody against VIPP1, Professor Martin Buck for providing the plasmid of pEC1 containing *pspA* from *E. coli*, and Rie Hijiya for technical assistance.

Received April 2, 2016; accepted May 9, 2016; published May 12, 2016.

LITERATURE CITED

Abdul-Gader A, Miles AJ, Wallace BA (2011) A reference dataset for the analyses of membrane protein secondary structures and transmembrane residues using circular dichroism spectroscopy. Bioinformatics **27:** 1630–1636

Ajees AA, Anantharamaiah GM, Mishra VK, Hussain MM, Murthy HM (2006) Crystal structure of human apolipoprotein A-I: insights into its protective effect against cardiovascular diseases. Proc Natl Acad Sci USA **103:** 2126–2131

Aseeva E, Ossenbühl F, Eichacker LA, Wanner G, Soll J, Vothknecht UC (2004) Complex formation of Vipp1 depends on its alpha-helical PspA-like domain. J Biol Chem **279:** 35535–35541

Dekov I, Tsonev T, Yordanov I (2000) Effects of water stress and high-temperature stress on the structure and activity of photosynthetic apparatus of *Zea mays* and *Helianthus annuus*. Photosynthetica **38:** 361–366

DeLisa MP, Lee P, Palmer T, Georgiou G (2004) Phage shock protein PspA of *Escherichia coli* relieves saturation of protein export via the Tat pathway. J Bacteriol **186:** 366–373

Engl C, Jovanovic G, Lloyd LJ, Murray H, Spitaler M, Ying L, Errington J, Buck M (2009) In vivo localizations of membrane stress controllers PspA and PspG in *Escherichia coli*. Mol Microbiol **73:** 382–396

Fuhrmann E, Bultema JB, Kahmann U, Rupprecht E, Boekema EJ, Schneider D (2009) The vesicle-inducing protein 1 from *Synechocystis sp. PCC 6803* organizes into diverse higher-ordered ring structures. Mol Biol Cell **20:** 4620–4628

Gao F, Wang W, Zhang W, Liu C (2015) α-Helical domains affecting the oligomerization of Vipp1 and its interaction with Hsp70/DnaK in Chlamydomonas. Biochemistry **54:** 4877–4889

Göhre V, Ossenbühl F, Crèvecoeur M, Eichacker LA, Rochaix JD (2006) One of two alb3 proteins is essential for the assembly of the photosystems and for cell survival in *Chlamydomonas*. Plant Cell **18:** 1454–1466

Heide H, Nordhues A, Drepper F, Nick S, Schulz-Raffelt M, Haehnel W, Schroda M (2009) Application of quantitative immunoprecipitation combined with knockdown and cross-linking to *Chlamydomonas* reveals the presence of vesicle-inducing protein in plastids 1 in a common complex with chloroplast HSP90C. Proteomics **9:** 3079–3089

Hennig R, Heidrich J, Saur M, Schmüser L, Roeters SJ, Hellmann N, Woutersen S, Bonn M, Weidner T, Markl J, Schneider D (2015) IM30 triggers membrane fusion in cyanobacteria and chloroplasts. Nat Commun **6:** 7018 10.1038/ncomms8018

Jouhet J, Gray JC (2009) Interaction of actin and the chloroplast protein import apparatus. J Biol Chem **284:** 19132–19141

Kleerebezem M, Crielaard W, Tommassen J (1996) Involvement of stress protein PspA (phage shock protein A) of *Escherichia coli* in maintenance of the protonmotive force under stress conditions. EMBO J **15:** 162–171

Kobayashi R, Suzuki T, Yoshida M (2007) *Escherichia coli* phage-shock protein A (PspA) binds to membrane phospholipids and repairs proton leakage of the damaged membranes. Mol Microbiol **66:** 100–109

Kroll D, Meierhoff K, Bechtold N, Kinoshita M, Westphal S, Vothknecht UC, Soll J, Westhoff P (2001) VIPP1, a nuclear gene of *Arabidopsis thaliana* essential for thylakoid membrane formation. Proc Natl Acad Sci USA **98:** 4238–4242

Li HM, Kaneko Y, Keegstra K (1994) Molecular cloning of a chloroplastic protein associated with both the envelope and thylakoid membranes. Plant Mol Biol **25:** 619–632

Lichtenthaler HK, Miehé J (1997) Fluorescence imaging as a diagnostic tool for plant stress. Trends Plant Sci **2:** 316–320

Lichtenthaler HK, Rinderle U (1988) The role of chlorophyll fluorescence in the detection of stress conditions in plants. C R C Crit Rev Anal Chem **1**(Suppl): 29–85

Liu C, Willmund F, Golecki JR, Cacace S, Hess B, Markert C, Schroda M (2007) The chloroplast HSP70B-CDJ2-CGE1 chaperones catalyse assembly and disassembly of VIPP1 oligomers in *Chlamydomonas*. Plant J **50:** 265–277

Liu C, Willmund F, Whitelegge JP, Hawat S, Knapp B, Lodha M, Schroda M (2005) J-domain protein CDJ2 and HSP70B are a plastidic chaperone pair that interacts with vesicle-inducing protein in plastids 1. Mol Biol Cell **16:** 1165–1177

Lo SM, Theg SM (2012) Role of vesicle-inducing protein in plastids 1 in cpTat transport at the thylakoid. Plant J **71:** 656–668

Ma SF, Lin CY, Chen YM (1990) Comparative studies of chilling stress on alterations of chloroplast ultrastructure and protein synthesis in the leaves of chilling sensitive (mungbean) and -insensitive (pea) seedlings. Bot Bull Acad Sin **31:** 263–272

McCain DC, Croxdale J, Markley JL (1989) Thermal damage to chloroplast envelope membranes. Plant Physiol **90:** 606–609

McDonald C, Jovanovic G, Ces O, Buck M (2015) Membrane stored curvature elastic stress modulates recruitment of maintenance proteins PspA and Vipp1. MBio **6:** e01188–15

Nordhues A, Schöttler MA, Unger AK, Geimer S, Schönfelder S, Schmollinger S, Rütgers M, Finazzi G, Soppa B, Sommer F, Mühlhaus T, Roach T, et al (2012) Evidence for a role of VIPP1 in the structural organization of the photosynthetic apparatus in Chlamydomonas. Plant Cell **24:** 637–659

Osadnik H, Schöpfel M, Heidrich E, Mehner D, Lilie H, Parthier C, Risselada HJ, Grubmüller H, Stubbs MT, Brüser T (2015) PspF-binding domain $PspA_{1-144}$ and the PspA·F complex: new insights into the coiled-coil-dependent regulation of AAA^+ proteins. Mol Microbiol **98:** 743–759

Otters S, Braun P, Hubner J, Wanner G, Vothknecht UC, Chigri F (2013) The first α-helical domain of the vesicle-inducing protein in plastids 1 promotes oligomerization and lipid binding. Planta **237:** 529–540

Provencher SW, Glöckner J (1981) Estimation of globular protein secondary structure from circular dichroism. Biochemistry **20:** 33–37

Receveur-Bréchot V, Bourhis JM, Uversky VN, Canard B, Longhi S (2006) Assessing protein disorder and induced folding. Proteins **62:** 24–45

Ross AH, Gericke A (2009) Phosphorylation keeps PTEN phosphatase closed for business. Proc Natl Acad Sci USA **106:** 1297–1298

Srivastava R, Pisareva T, Norling B (2005) Proteomic studies of the thylakoid membrane of *Synechocystis sp. PCC 6803*. Proteomics **5:** 4905–4916

Standar K, Mehner D, Osadnik H, Berthelmann F, Hause G, Lünsdorf H, Brüser T (2008) PspA can form large scaffolds in *Escherichia coli*. FEBS Lett **582:** 3585–3589

Sun X, Rikkerink EHA, Jones WT, Uversky VN (2013) Multifarious roles of intrinsic disorder in proteins illustrate its broad impact on plant biology. Plant Cell **25:** 38–55

Tanaka A (2007) Photosynthetic activity in winter needles of the evergreen tree *Taxus cuspidata* at low temperatures. Tree Physiol **27:** 641–648

Tolleter D, Hincha DK, Macherel D (2010) A mitochondrial late embryogenesis abundant protein stabilizes model membranes in the dry state. Biochim Biophys Acta **1798:** 1926–1933

Tuba Z, Lichtenthaler HK, Csintalan Z, Nagy Z, Szente K (1994) Reconstitution of chlorophylls and photosynthetic CO_2 assimilation upon rehydration of the desiccated poikilochlorophyllous plant *Xerophyta scabrida* (Pax). Th Dur et Schinz Planta **192:** 414–420

van Stokkum IHM, Spoelder HJW, Bloemendal M, van Grondelle R, Groen FCA (1990) Estimation of protein secondary structure and error analysis from circular dichroism spectra. Anal Biochem **191:** 110–118

Vazquez F, Ramaswamy S, Nakamura N, Sellers WR (2000) Phosphorylation of the PTEN tail regulates protein stability and function. Mol Cell Biol **20:** 5010–5018

Vothknecht UC, Otters S, Hennig R, Schneider D (2012) Vipp1: a very important protein in plastids?! J Exp Bot **63:** 1699–1712

Ward JJ, Sodhi JS, McGuffin LJ, Buxton BF, Jones DT (2004) Prediction and functional analysis of native disorder in proteins from the three kingdoms of life. J Mol Biol **337:** 635–645

Westphal S, Heins L, Soll J, Vothknecht UC (2001) Vipp1 deletion mutant of *Synechocystis*: a connection between bacterial phage shock and thylakoid biogenesis? Proc Natl Acad Sci USA **98:** 4243–4248

Whitmore L, Wallace BA (2008) Protein secondary structure analyses from circular dichroism spectroscopy: methods and reference databases. Biopolymers **89:** 392–400

Yamaguchi S, Reid DA, Rothenberg E, Darwin AJ (2013) Changes in Psp protein binding partners, localization and behaviour upon activation of the *Yersinia enterocolitica* phage shock protein response. Mol Microbiol **87:** 656–671

Zhang L, Kato Y, Otters S, Vothknecht UC, Sakamoto W (2012) Essential role of VIPP1 in chloroplast envelope maintenance in *Arabidopsis*. Plant Cell **24:** 3695–3707

Zhang LG, Kusaba M, Tanaka A, Sakamoto W (2016) Protection of chloroplast membranes by VIPP1 rescues aberrant seedling development in Arabidopsis *nyc1* mutant. Front Plant Sci **7:** 533

Zhang L, Sakamoto W (2015) Possible function of VIPP1 in maintaining chloroplast membranes. Biochim Biophys Acta **1847:** 831–837

Zhang L, Sakamoto W (2013) Possible function of VIPP1 in thylakoids: protection but not formation? Plant Signal Behav **8:** e22860

Zhang S, Shen G, Li Z, Golbeck JH, Bryant DA (2014) Vipp1 is essential for the biogenesis of Photosystem I but not thylakoid membranes in *Synechococcus* sp. PCC 7002. J Biol Chem **289:** 15904–15914